AIP | Applied Physics Letters

Pressure tuning the lattice and optical response of silver sulfide

Zhao Zhao, Hua Wei, and Wendy L. Mao

Citation: Applied Physics Letters **108**, 261902 (2016); doi: 10.1063/1.4954801
View online: http://dx.doi.org/10.1063/1.4954801
View Table of Contents: http://scitation.aip.org/content/aip/journal/apl/108/26?ver=pdfcov
Published by the AIP Publishing

Pressure tuning the lattice and optical response of silver sulfide

Zhao Zhao,[1,a)] Hua Wei,[2] and Wendy L. Mao[3,4]
[1]*Department of Physics, Stanford University, Stanford, California 94305, USA*
[2]*Scintillation Materials Research Center, Department of Materials Science and Engineering, University of Tennessee, Knoxville, Tennessee 37996, USA*
[3]*Stanford Institute for Materials and Energy Sciences, SLAC National Accelerator Laboratory, Menlo Park, California 94025, USA*
[4]*Department of Geological Sciences, Stanford University, Stanford, California 94305, USA*

(Received 25 May 2016; accepted 14 June 2016; published online 27 June 2016)

Binary transition metal chalcogenides have attracted increasing attention for their unique structural and electronic properties. High pressure is a powerful tool for tuning the lattice and electronic structure of transition metal chalcogenides away from their pristine states. In this work, we systematically studied the *in situ* structural and optical behavior of silver sulfide (Ag_2S) under pressure by synchrotron X-ray diffraction and infrared spectroscopy measurements in a diamond anvil cell. Upon compression, Ag_2S undergoes structural symmetrization accompanied by a series of structural transitions while the crystallographic inequivalence of the two Ag sites is maintained. Electronically, pressure effectively tunes the ambient semiconducting Ag_2S into a metal at ~22 GPa. Drude model analysis shows that the optical conductivity evolves significantly, reaching the highest value of 100 $\Omega^{-1}\,cm^{-1}$ at ~40 GPa. Our results highlight the structural and electronic tunability of silver chalcogenides as a function of pressure and suggest the potential of Ag_2S as a platform for developing optical and opto-electronic applications. *Published by AIP Publishing.*
[http://dx.doi.org/10.1063/1.4954801]

Binary transition metal chalcogenides have attracted significant research and industrial interest in recent years. For example, the discovery of topological insulators Bi_2Te_3 and Bi_2Se_3 has opened up novel states of matter for condensed matter research.[1–3] The resurgent interest on layered transition-metal chalcogenides WX_2 and MoX_2 (X = S, Se, and Te) presents promising opportunities in developing next-generation electronics and transistors.[4–7] Silver chalcogenides Ag_2X is another group of interest. Ag_2Se and Ag_2Te with bulk band-gaps of ~0.1 to 0.2 eV were proposed as new 3D topological insulators[8] possible for spintronic applications based on their highly anisotropic Dirac cones.[9] Experimental evidence supporting metallic surface states has been found in the case of Ag_2Te.[10,11] In contrast, Ag_2S is a semiconductor with a band-gap of ~1 eV.[12,13] Ag_2S enables fabrication of quantized conductance atomic switches that can largely overcome the limitation of current semiconductor devices.[14] In addition, Ag_2S quantum dots can be applied in high sensitivity medical imaging.[15]

The ability to tune the electronic structures of semiconductors away from their pristine states is fundamental to semiconductor research, because this capability could lead to novel electronic and opto-electronic functionalities. For Ag_2X, a variety of experimental techniques have been employed to engineer their electronic structures and band-gaps. Two prominent examples involve tuning their dimensionality via film thickness and particle size.[16–20] By varying the thickness, its activation gap was effectively tuned.[16] By changing the particle size, its optical band-gap could also be engineered.[17–19]

Pressure is a powerful tool in modifying the atomic arrangement and thus to dramatically alter material's electronic structure and physical properties. Previous high pressure studies on transition metal chalcogenides have unveiled a variety of new phases and interesting behaviors. Studies on Bi_2Te_3 and Bi_2Se_3 showed that pressure induced transformations into new crystal structures with different electronic structures.[21–23] Studies on MoS_2 and $MoSe_2$ show that pressure can continuously tune their band-gap and lead to metallization.[24,25] For Ag_2X, earlier work on Ag_2Te and Ag_2Se showed that pressure induced abrupt semiconductor to metal transitions associated with structural transitions at ~3 GPa and ~8 GPa, respectively.[26–28]

For Ag_2S, a previous study up to ~20 GPa showed that it undergoes phase transitions from the monoclinic phase I to an orthorhombic phase II at 5.4 GPa and then to another monoclinic phase III at 10.6 GPa.[29] Interestingly, one high symmetry orthorhombic phase (space group *Pnma*) was predicted at higher pressure. Yet this phase was not observed due to the limited pressure range in their experiments. Electrical transport measurements up to ~19 GPa combined with first-principles calculations showed that Ag_2S remained semiconducting while exhibiting dramatic changes in majority carrier concentration and mobility.[30]

In this work, we aimed to (1) explore possible structural transitions at higher pressure, (2) clarify the structural connections among the different phases, and (3) determine how pressure tunes the optical response which relates to the evolution of the band-gap and optical conductivity. We performed *in situ* synchrotron angle dispersive powder X-ray diffraction (XRD) experiments up to ~50 GPa and infrared (IR) spectroscopy experiments up to ~40 GPa (Fig. 1(a)), and presented detailed structural and optical analyses on behavior of compressed Ag_2S.

The Ag_2S sample (purity higher than 99%, product number 241474, Lot number MKBQ6420V) was purchased

a)E-mail: zhaozhao@stanford.edu

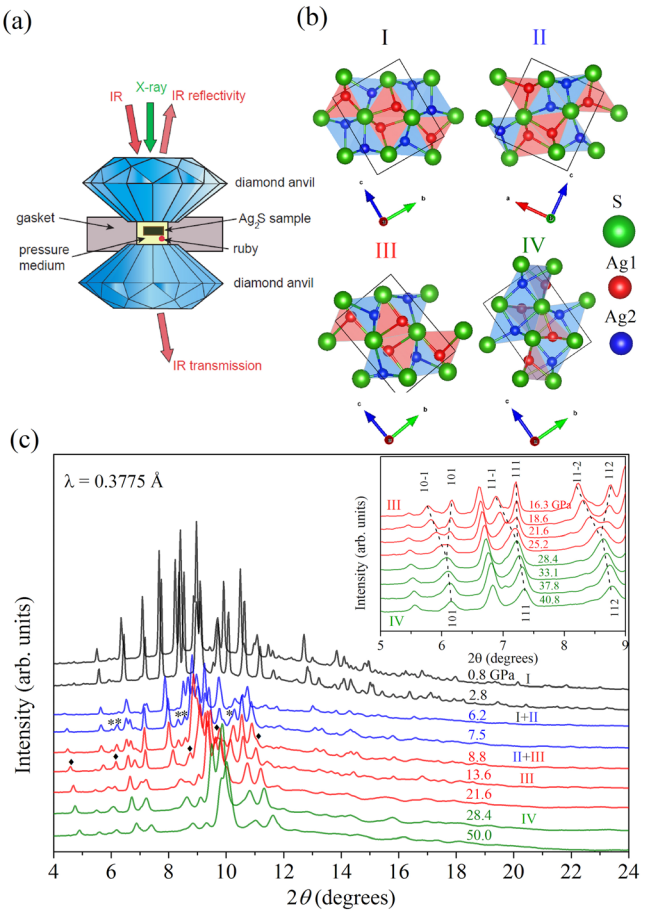

FIG. 1. (a) Experimental set up for high pressure X-ray and IR measurements. (b) Crystal structures for the four phases of Ag_2S under pressure, where two distinctive Ag sites are observed. (c) Representative high pressure XRD patterns with $\lambda = 0.3775$ Å. Numbers on the right are pressures in units of GPa. New diffraction peaks in phase II are shown by stars and phase III by diamonds. Inset of (c) shows the symmetrization from phase III to phase IV.

from Sigma-Aldrich. The sample was checked by XRD, Inductively Coupled Plasma Mass Spectrometry, and X-ray Photoemission Spectroscopy. Symmetric DACs with 300 μm culet size were used. A tungsten thin foil was used as the gasket and a 120 μm diameter hole was drilled as the sample chamber. The gasket was pre-indented to a thickness of ~40 μm. Ruby spheres were used for determining pressure for all of the measurements. Silicone oil was used as the pressure transmitting medium for the XRD measurements. Two sets of *in situ* angle dispersive XRD data were collected at 12.2.2 of Advanced Light Source (ALS), Lawrence Berkeley National Laboratory (LBNL), with wavelengths of 0.3775 Å and 0.4959 Å. Rietveld fitting was performed by GSAS-EXPGUI package.[31] A Birch–Murnaghan (BM) Equation of State (EOS) is employed to fit the experimental P-V relationship, using EOSFit V5.2 software.[32] The uncertainties of volumes given by GSAS are included in the fitting for all four phases.

For the IR measurements, KBr was used as the pressure transmitting as it is IR transparent. Type IIa diamonds which are almost free of nitrogen impurities were used.[33] High-pressure IR measurements were conducted in beamline U2A of the National Synchrotron Light Source (NSLS), Brookhaven National Laboratory (BNL). Both reflectance and transmittance were measured in the spectral range between 600 and 8000 cm^{-1} with the resolution of 4 cm^{-1}. To convert reflectivity from the Ag_2S/diamond interface to the Ag_2S/vacuum interface, the correction according to Fresnel's formula is employed.[34] A Drude–Lorentz model with Kramers–Kronig relation was applied for the IR reflectivity data using iterative fitting in RefFit software.[35] More details can be found in the supplementary material.[36]

Figs. 1(b) and 1(c) show the four crystal structures of Ag_2S and representative XRD pattern collected during compression. The lowest pressure measurement at 0.8 GPa is consistent with the ambient condition structure. When increasing the pressure to 5.1 GPa, phase II is observed to coexist with phase I. At 8.8 GPa, new peaks from phase III appear. At 28.4 GPa, some peaks merge together, suggesting the transition from phase III to phase IV (see the inset of Fig. 1(c)). Decompression cycles show that all structural transitions are reversible. Representative Rietveld refinement profiles and crystallographic information are shown in Fig. S1 and Table S1 of the supplementary material.[36]

By combining the Rietveld refinement results, we obtained the evolution of the unit cell volume and cell parameters in Fig. 2. Phase I has a distorted anti-$PbCl_2$ type structure (Figure 1(b)), where Ag1 and Ag2 atoms are both four-fold coordinated. Ag1 is closer to one S layer on the (010) plane, while Ag2 is more in between the two S layers.[37,38] At

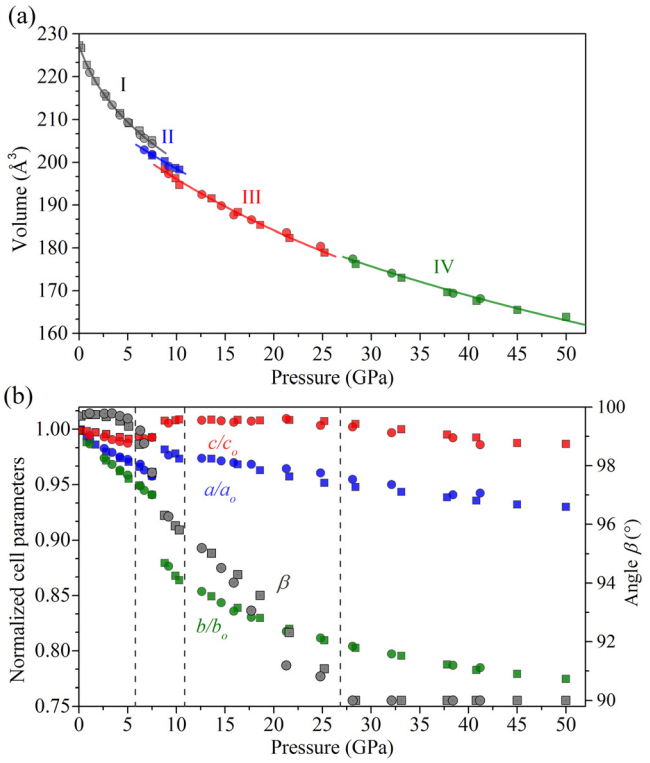

FIG. 2. (a) Pressure-volume EOS of Ag_2S. Circles and squares represent data from two separate runs. The curves are BM-EOS for each phase where phase I was fit by a third-order EOS and the rest by second-order EOS. (b) Normalized cell parameters and angle for phases I, III, and IV as a function of pressure. Phase II is not plotted here because it has an orthorhombic structure and does not fit in with the continuous decrease of angle. Phase IV is converted from *Pnma* to *Pmnb* for better comparison. Uncertainties given by GSAS-EXPGUI are smaller than marker sizes.

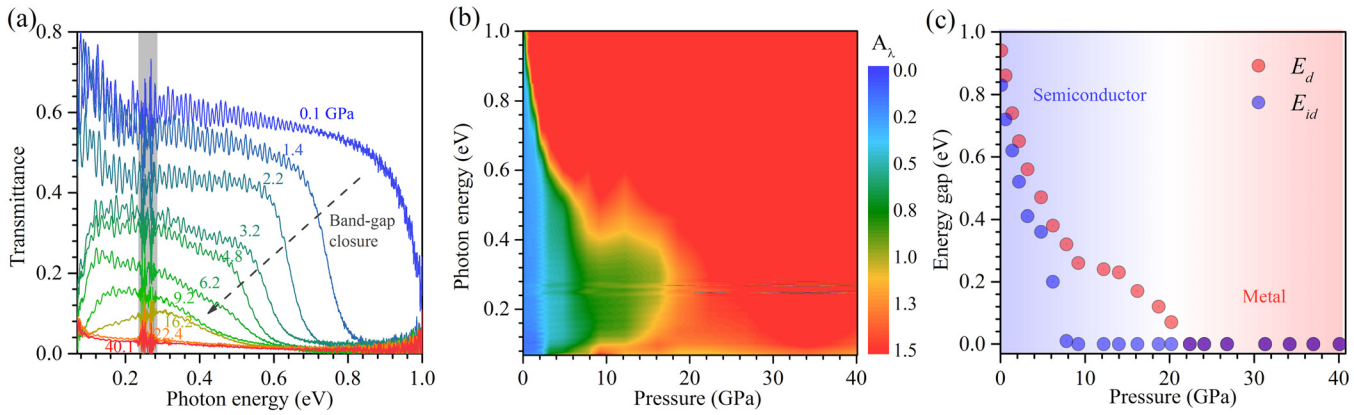

FIG. 3. (a) Representative IR transmittance spectra at various pressures. The 0.23–0.28 eV region is obscured by absorption of the diamonds in the DAC. (b) Pressure-photon energy-optical density mapping. (c) Evolution of band-gaps with pressure.

~5 GPa, a decrease of β angle from approximately 99° to 98° and a concurrent change of compressibility in the c direction are observed. The Ag-S distance decreases quickly while the Ag-Ag distance remains almost constant before 5 GPa, while after 5 GPa all atomic distances decrease at similar rates.[29] Fig. 2(b) shows that among the three axes, the b direction is the most compressible. Table S2 presents the EOS of all phases. For phase I, $K_0 = 34$ (2) GPa and $K' = 17$ (2), consistent with the previous study.[29] The large K' indicates a strong change in compressibility of the monoclinic structure phase I, where it changes from highly compressible to much less compressible with pressure.

Phase II is orthorhombic (space group $P2_12_12_1$) and isostructural to the ambient condition structure of Ag_2Se.[29,30] Note that pure phase II was not observed in any of the runs. This supports previous calculations showing that phase I and phase II are energetically close. Possibly, slight disturbance such as small deviatoric stress or non-hydrostaticity may render phase II unfavorable to phase I, and therefore lead to a mixture of two phases. In phase II, two Ag sites are still observed within the structure. S layers are formed in the (001) plane, and Ag1 is still closer to the plane when compared with Ag2. Ag1 is four-fold coordinated to form distorted tetrahedra. Differently, Ag2 increases from four-fold to five-fold coordinated to form pyramids.

The $P2_1/n$ phase III structure is isosymmetric to phase I structure, seen in Fig. 1(b). In terms of cell parameters, a and c both expanded while b contracted from phase I to phase III, The coordination of Ag2 is maintained at five (pyramid-like structure), but the coordination of Ag1 increase from four to five as Ag1 is almost on the (010) plane formed by S to form trigonal bipyramidal. The incompressibility of the c axis is closely related to the strong decrease of β angle. As pressure increases, strong distortions of Ag-S polyhedra occur due to increasing ionic interactions. We also fitted the EOS of phase III yielding $V_0 = 213.0$ (7) Å^3, $K_0 = 102$ (4) GPa.

When pressure reached ~28 GPa, we experimentally discovered the *Pnma* phase that was predicted in previous calculations.[29] The structural symmetrization from phase III to phase IV is supported by the continuous decrease of β to ~90° and continuous lattice contraction. In this high symmetry phase IV structure, two different Ag sites persist where Ag1 forms trigonal bipyramids and Ag2 forms pyramids with nearby S atoms. It should be noted that the crystallographic differences of the two Ag sites persisted to the highest pressure studied. The EOS parameters of phase IV are $V_0 = 209$ (4) Å^3 and $K_0 = 123$ (15) GPa.

The lattice response of Ag_2S under pressure will also affect its electronic structure and optical properties. We performed *in situ* IR reflectivity and transmission spectroscopy measurements up to ~40 GPa. Fig. 3 presents the measured synchrotron IR transmittance spectra and analyses. At the lowest pressure of 0.1 GPa, the spectrum (Fig. 3(a)) shows an abrupt change at the absorption edge ~0.9 eV and an IR transmission window at energy region below it. This agrees with the band-gap being ~1 eV at ambient pressure.[12,13] As the pressure increases, the transmission window keeps collapsing at lower energies, which indicates the narrowing of band-gap. At 22.4 GPa, nearly zero transmission is observed between 0.1 and 1.0 eV, suggesting metallization. Further increase pressure to the highest pressure of 40.1 GPa does not change the IR spectrum. We can also interpret the IR data by the optical density (OD or A_λ), where A_λ is defined as the logarithm (log) of T. As seen from Fig. 3(b) for the pressure-photon-energy-A_λ map, a crossover of low A_λ (semiconducting state) to high A_λ (metallic state) occurs at ~20 GPa.

For more detailed analysis on the electronic structure, we employed empirical models to fit the optical band-gaps. For a direct band-gap semiconductor, the absorption coefficient is proportional to the root of the energy difference of the photon energy and band-gap, $\alpha \propto (h\nu - E_{id})^{1/2}/h\nu$. For an indirect band-gap semiconductor, a square law is followed where $\alpha \propto (h\nu - E_d)^2/h\nu$. We therefore perform linear extrapolations of $(A_\lambda h\nu)^{1/2}$ and $(A_\lambda h\nu)^2$ to determine the direct band-gap E_d and indirect band-gap E_{id}. Representative extrapolations are shown in Fig. S2. Energy gaps as a function of pressure are shown in Fig. 3(c). As pressure increases, both E_{id} and E_d unanimously decrease, supporting the band-gap narrowing. Consider that Ag_2S is calculated to be a direct band-gap semiconductor, E_d should more accurately represent the electronic band-gap of Ag_2S. At pressure above 22 GPa, the E_d effectively becomes zero.

To better probe the optical response as a function of pressure, we simultaneously measured the IR reflectivity at each pressure (Fig. 4(a)). Below 9 GPa, the spectrum appears flat and featureless. At 9.2 GPa, the reflectivity starts to transform where

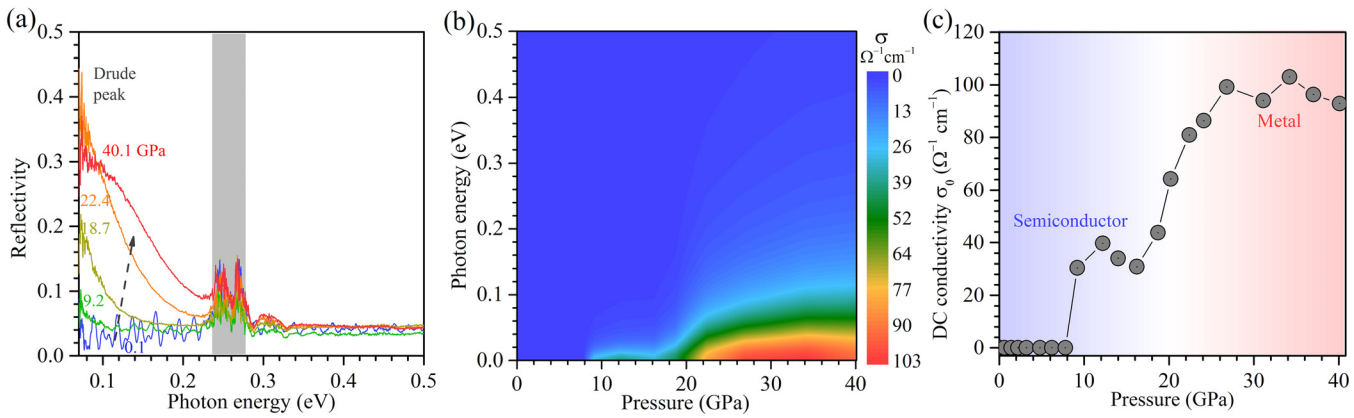

FIG. 4. (a) Representative IR reflectance spectra at various pressures. The 0.23–0.28 eV region is obscured by absorption of the diamonds in the DAC. (b) Pressure-photon energy-optical conductivity (σ) mapping. (c) Evolution of DC conductivity (σ_0) with pressure.

the low energies part increases in intensities. At 22.4 GPa, the Drude mode appears, which is a strong evidence of metallization. To quantitatively characterize the optical response, we derived the optical conductivity σ from the Kramers–Kronig analysis. Representative fitting is shown in Fig. S3. For consistency, a Drude model was used in all of the fittings. The results are shown in Fig. 4(b) and a clear crossover from semiconducting to metallic can be seen. We further plot the zero frequency (DC) conductivity of Ag_2S in Fig. 4(c). Clear features can be seen: the DC conductivity appears at above 9 GPa with values of about 30 to 40 $\Omega^{-1}\,cm^{-1}$. From 18 to 26 GPa, the DC conductivity strongly increases to about 100 $\Omega^{-1}\,cm^{-1}$ and maintains this value up to the highest pressure studied.

An important question worth discussing is whether the metallization of Ag_2S is related to any structural transitions. The phase II to III transition can be ruled out because it occurs far below the metallization pressure. However, the phase III to IV transition occurs between 25 and 28 GPa, slightly higher than the electronic transition at 22 GPa. We propose two possibilities here. One scenario is that the metallization of Ag_2S accompanies the phase III to IV transition, where the difference in pressure media (KBr in the IR experiments and silicone oil in the XRD experiments) leads to the apparent difference in the simultaneous phase III to IV and semiconductor to metal transition. The other scenario is that the metallization occurs within phase III. During the structural symmetrization, the band-gap of phase III decreases and reaches zero. Considering that the structural evolution from phase III to IV is smooth, the electronic structure of phase IV may be also similar to pressurized phase III and thus be metallic. In either case, the metallization of Ag_2S is a sluggish process because of the continuous structural change.

Among the group of silver chalcogenides, pressure has been found to induce a series of structural transitions.[21,22,26,27,39] For Ag_2Se and Ag_2Te, the abrupt semiconductor to metal transition relates to first-order structural transitions with large changes in their crystal structures.[26,27] However, in the case of Ag_2S, the band-gap varies smoothly when undergoing structural transitions. This suggests that among Ag_2X, Ag_2S may be a more suitable materials systems for developing optical and optoelectronics applications among Ag_2X. The phase II of Ag_2S is isostructural to the ambient structure of Ag_2Se; therefore, they are likely to have a similar electronic structure. Considering that Ag_2Se is a potential topological insulator with inverted band structure[28] and Ag_2S's band-gap becomes as small as ~0.4 eV at 5 GPa, there lies the possibility that phase II of Ag_2S is also a topological insulator. Future calculations would be useful to test this novel scenario.

In summary, we studied the high pressure structural and optical behavior of Ag_2S by *in situ* angle dispersive XRD and IR experiments. The structural connections and symmetrization from phase I to phase IV are presented. Pressure continuously tuned semiconducting Ag_2S into a metal at ~22 GPa, while its DC conductivity reached the highest value (100 $\Omega^{-1}\,cm^{-1}$) at ~40 GPa. Our results highlight the dramatic ability of pressure for tuning the structural and electronic state of silver chalcogenides and suggest Ag_2S for possible optical and optoelectronic applications.

We thank Jinyuan Yan at ALS and Zhenxian Liu at NSLS for their technical assistance. Zhao Zhao and Wendy L. Mao are supported by the Department of Energy (DOE), Basic Energy Sciences (BES), Materials Sciences and Engineering Division, under Contract No. DE-AC02-76SF00515. ALS is supported by DOS-BES, DE-AC02-05CH11231. U2A is supported by COMPRES under NSF Cooperative Agreement Nos. EAR 11-57758 and DOE-NNSA DE-FC03-03N00144, CDAC. NSLS is supported by DOE-BES, DE-AC02-98CH10886.

[1]Y. L. Chen, J. G. Analytis, J.-H. Chu, Z. K. Liu, S.-K. Mo, X. L. Qi, H. J. Zhang, D. H. Lu, X. Dai, Z. Fang, S. C. Zhang, I. R. Fisher, Z. Hussain, and Z.-X. Shen, Science **325**, 178 (2009).
[2]H. Zhang, C.-X. Liu, X.-L. Qi, X. Dai, Z. Fang, and S.-C. Zhang, Nat. Phys. **5**, 438 (2009).
[3]K. He, Y. Zhang, C.-Z. Chang, C.-L. Song, L.-L. Wang, X. Chen, J.-F. Jia, Z. Fang, X. Dai, W.-Y. Shan, S.-Q. Shen, Q. Niu, X.-L. Qi, S.-C. Zhang, X.-C. Ma, and Q.-K. Xue, Nat. Phys. **6**, 584 (2010).
[4]J. N. Coleman, M. Lotya, A. O'Neill, S. D. Bergin, P. J. King, U. Khan, K. Young, A. Gaucher, S. De, R. J. Smith, I. V. Shvets, S. K. Arora, G. Stanton, H.-Y. Kim, K. Lee, G. T. Kim, G. S. Duesberg, T. Hallam, J. J. Boland, J. J. Wang, J. F. Donegan, J. C. Grunlan, G. Moriarty, A. Shmeliov, R. J. Nicholls, J. M. Perkins, E. M. Grieveson, K. Theuwissen, D. W. McComb, P. D. Nellist, and V. Nicolosi, Science **331**, 568 (2011).
[5]Q. H. Wang, K. Kalantar-Zadeh, A. Kis, J. N. Coleman, and M. S. Strano, Nat. Nanotechnol. **7**, 699 (2012).
[6]X. Li, F. Zhang, and Q. Niu, Phys. Rev. Lett. **110**, 066803 (2013).
[7]M. Chhowalla, H. S. Shin, G. Eda, L.-J. Li, K. P. Loh, and H. Zhang, Nat. Chem. **5**, 263 (2013).

[8]W. Zhang, R. Yu, W. Feng, Y. Yao, H. Weng, X. Dai, and Z. Fang, Phys. Rev. Lett. **106**, 156808 (2011).
[9]F. Virot, R. Hayn, M. Richter, and J. van den Brink, Phys. Rev. Lett. **106**, 236806 (2011).
[10]S. Lee, J. In, Y. Yoo, Y. Jo, Y. C. Park, H.-J. Kim, H. C. Koo, J. Kim, B. Kim, and K. L. Wang, Nano Lett. **12**, 4194 (2012).
[11]A. Sulaev, P. Ren, B. Xia, Q. H. Lin, T. Yu, C. Qiu, S. Y. Zhang, M. Y. Han, Z. P. Li, W. G. Zhu, Q. Wu, Y. P. Feng, L. Shen, S. Q. Shen, and L. Wang, AIP Adv. **3**, 032123 (2013).
[12]C. Sugiura, M. Kitamura, S. Muramatsu, S. Shoji, S. Kojima, Y. Tada, I. Umezu, and T. Arai, Jpn. J. Appl. Phys., Part 1 **27**, 1216 (1988).
[13]R. Zamiri, H. A. Ahangar, A. Zakaria, G. Zamiri, and M. Shabani, Chem. Cent. J. **9**, 28 (2015).
[14]K. Terabe, T. Hasegawa, T. Nakayama, and M. Aono, Nature **433**, 47 (2005).
[15]G. Hong, J. Robinson, Y. Zhang, S. Diao, A. L. Antaris, Q. Wang, and H. Dai, Angew. Chem., Int. Ed. **51**, 9818 (2012).
[16]V. D. Das and D. Karunakaran, Phys. Rev. B **39**, 10872 (1989).
[17]Y.-P. Gu, R. Cui, Z.-L. Zhang, Z.-X. Xie, and D.-W. Pang, J. Am. Chem. Soc. **134**, 79 (2012).
[18]A. Sahu, A. Khare, D. D. Deng, and D. J. Norris, Chem. Commun **48**, 5458 (2012).
[19]C.-N. Zhu, P. Jiang, Z.-L. Zhang, D.-L. Zhu, Z.-Q. Tian, and D.-W. Pang, ACS Appl. Mater. Interfaces **5**, 1186 (2013).
[20]Y. Zhang, Y. Liu, C. Li, X. Chen, and Q. Wang, J. Phys. Chem. C **118**, 4918 (2014).
[21]L. Zhu, H. Wang, Y. Wang, J. Lv, Y. Ma, Q. Cui, Y. Ma, and G. Zou, Phys. Rev. Lett. **106**, 145501 (2011).
[22]R. Vilaplana, D. Santamaría-Pérez, O. Gomis, F. J. Manjón, J. González, A. Segura, A. Muñoz, P. Rodríguez-Hernández, E. Pérez-González, V. Marín-Borrás, V. Muñoz-Sanjose, C. Drasar, and V. Kucek, Phys. Rev. B **84**, 184110 (2011).
[23]A. Segura, V. Panchal, J. F. Sánchez-Royo, V. Marín-Borrás, V. Muñoz-Sanjosé, P. Rodríguez-Hernández, A. Muñoz, E. Pérez-González, F. J. Manjón, and J. González, Phys. Rev. B **85**, 195139 (2012).
[24]A. P. Nayak, S. Bhattacharyya, J. Zhu, J. Liu, X. Wu, T. Pandey, C. Jin, A. K. Singh, D. Akinwande, and J.-F. Lin, Nat. Commun. **5**, 3731 (2014).
[25]Z. Zhao, H. Zhang, H. Yuan, S. Wang, Y. Lin, Q. Zeng, G. Xu, Z. Liu, G. K. Solanki, K. D. Patel, Y. Cui, H. Y. Hwang, and W. L. Mao, Nat. Commun. **6**, 7312 (2015).
[26]M. D. Banus and M. C. Finn, J. EIectrochem. Soc. **116**, 91 (1969).
[27]Z. Zhao, S. Wang, H. Zhang, and W. L. Mao, Phys. Rev. B **88**, 024120 (2013).
[28]Z. Zhao, S. Wang, A. R. Oganov, P. Chen, Z. Liu, and W. L. Mao, Phys. Rev. B **89**, 180102(R) (2014).
[29]D. Santamaría-Pérez, M. Marqués, R. Chuliá-Jordán, J. M. Menendez, O. Gomis, J. Ruiz-Fuertes, J. A. Sans, D. Errandonea, and J. M. Recio, Inorg. Chem. **51**, 5289 (2012).
[30]J. Zhang, C. Liu, X. Zhang, F. Ke, Y. Han, G. Peng, Y. Ma, and C. Gao, Appl. Phys. Lett. **103**, 082116 (2013).
[31]B. H. Toby, J. Appl. Crystallogr. **34**, 210 (2001).
[32]R. J. Angel, EosFit v5.2.
[33]H. Okamura, M. Matsunami, R. Kitamura, S. Ishida, A. Ochiai, and T. Nanba, J. Phys.: Conf. Ser. **215**, 012051 (2010).
[34]G. Burns, *Solid State Physics* (Academic Press, New York, 1985).
[35]A. B. Kuzmenko, Rev. Sci. Instrum. **76**, 83108 (2005).
[36]See supplementary material at http://dx.doi.org/10.1063/1.4954801 for more details about experimental set up, X-ray structural refinement, and infrared fitting.
[37]A. Frueh, Acta Crystallogr. **10**, 764 (1957).
[38]R. Y. Wang, R. Tangirala, S. Raoux, J. L. Jordan-Sweet, and D. J. Milliron, Adv. Mater. **24**, 99 (2012).
[39]J. Zhao, H. Liu, L. Ehm, Z. Chen, S. Sinogeikin, Y. Zhao, and G. Gu, Inorg. Chem. **50**, 11291 (2011).